Materials Physics and Mechanics 22 (2015) 1-14 Received: July 26, 2014

REFLECTION OF PLANE WAVES IN TRANSVERSELY ISOTROPIC MICROPOLAR VISCOTHERMOELASTIC SOLID

Rajneesh Kumar[1], K.D. Sharma[2*], S.K. Garg[3]

[1]Department of Mathematics, Kurukshetra University Kurukshetra, Kurukshetra, India

[2]Department of Mathematics, Swami Devi Dyal Institute of Engineering &Technology, Barwala, India

[3]Department of Mathematics, Deenbandhu Chhotu Ram University, Murthal (Sonipat), India

*e-mail: kd_sharma33@rediffmail.com

Abstract. The reflection of plane waves at the free surface of transversely isotropic micropolar viscothermoelastic medium is investigated. It is found that there exist four types of plane waves in transversely isotropic micropolar viscothermoelastic medium, namely quasi-longtitudinal displacement (qLD), quasi-transverse displacement (qTD), quasi-transverse microrotaional (qTM), quasi-thermal (qT) wave. The amplitude ratios corresponding to reflected waves are obtained numerically when different waves are incident. Numerically simulated results are depicted graphically with respect to the frequency. The effect of viscosity on the amplitude ratios are shown graphically for specific model. Some particular results are also deduced.

1. Introduction

Viscoelastic materials are those for which the relationship between stress and strain depends on time. All materials exhibit some viscoelastic response. In common metals such as steel, aluminum, copper etc. At room temperature and small strain, the behavior does not deviate much from linear elasticity. Synthetic polymer, wood as well as metals at high temperature display significant viscoelastic effects. With the rapid development of polymer science and plastic industry, as well as the wide use of materials under high temperature in modern technology and application of biology and geology in engineering, the theoretical study and applications in viscoelastic materials has become an important task for solid mechanics.

The Kelvin-Voigt (1887) [1] model is one of the macroscopic mechanical models often used to describe the viscoelastic behavior of the material. This model represents the delayed elastic response subjected to stress when the deformation is time dependent but recoverable. The dynamical interaction of thermal and mechanical fields in solids has great practical applications in modern aeronautics, astronautics, nuclear reactors and high energy particle accelerators.

Eringen (1967) [2] extended the theory of micropolar elasticity to obtain linear constitutive theory for micropolar material possessing internal friction. A problem on micropolar viscoelastic waves has been discussed by McCarthy and Eringen (1969) [3]. Kumar, Gogna and Debnath (1990) [4] studied Lamb's plane problem in a micropolar viscoelastic half-space with stretch. Biswas, Sengupta and Debnath (1996) [5] studied the axisymmetric problems of wave propagation under the influence of gravity in a micropolar viscoelastic semi-infinite medium when a time varying axisymmetric loading has been applied on the surface of the medium. De Cicco and Nappa (1998) [6] discussed the problem of Saint Venant's principle for micropolar viscoelastic bodies.

Kumar and Singh (1998) [7] obtained the reflection and refraction coefficient of plane waves at an interface between micropolar elastic solid and viscoelastic solid. Kumar and Singh (2000) [8] studied reflection of plane waves at a planer viscoelastic micropolar interface. Singh (2000) [9] obtained the reflection and transmission at the interface between a liquid and micropolar viscoelastic solid with stretch. Kumar (2000) [10] studied wave propagation in micropolar viscoelastic generalized thermoelastic solid. El-Karamany (2002) [11] proved the uniqueness and reciprocity theorems in a generalized linear micropolar thermoviscoelasticity. El-Karamany (2004) [12] presented boundary integral equation formulation for generalized micropolar thermoelastic media. Kumar and Singh (2005) [13] investigated an axisymmetric problem in microstretch viscoelastic solid. Oathman and Song (2007) [14] investigated the reflection and transmission of thermoviscoelastic waves at the interface between two micropolar viscoelastic media without energy dissipation. Kumar and Sharma (2007) [15] investigated effect of viscosity on wave propagation between two micropolar thermoviscoelastic solid with two relaxation times having imperfect boundary.

Kumar and Partap (2008) [16] investigated analysis of free vibrations for Rayleigh Lamb waves in a micropolar viscoelastic plate. Sharma and Sharma (2008) [17] investigated propagation of waves in micropolar viscoelastic generalized thermoelastic solids having interfacial imperfections. Kumar and Sharma (2009) [18] studied the effect of viscosity and stiffness on wave propagation in micropolar viscoelastic media. Kumar and Partap (2010) [19] investigated free vibration analysis of waves in a microstrech viscoelastic layer. El-Karamany (2011) [20] proved the reciprocal theorem and established convulational variation principal for two temperature linearly isotropic and inhomogeneous thermoviscoelastic solids. Mondal and Mukhopadhyay (2012) [21] studied the effect of two temperatures on thermoviscoelastic problem with rheological properties. Kumar, Sharma and Garg (2012) [22] investigated the effect of viscosity on plane wave propagation in heat conducting transversely isotropic micropolar viscoelastic half space. Kumar, Chawla and Abbas (2012) [23] investigated the effect of viscosity on wave propagation in anisotropic thermoelastic medium with three-phase-lag model. Sharma, Sharma and Dhaliwal (2012) [24] presented three dimensional free vibration analysis of a viscothermoelastic hollow sphere. Sharma, Sharma and Bhargava (2013) [25] investigated the effect of viscosity on wave propagation in anisotropic thermoelastic with Green-Naghdi theory Type-II and Type-III.

Kumar, Sharma and Garg (2014) [26] studied the effect of two temperatures on reflection coefficient in micropolar thermoelastic with and without energy dissipation media. Kumar, Kaur and Rajvanshi (2014) [27] investigated reflection and transmission of plane wave at an interface between two micropolar thermoelastic half-space with different micropolarity and thermoelastic properties. Kumar and Kaur (2014) [28] discussed the reflection and refraction of waves at the interface of an elastic solid and microstrech thermoelastic solid with microtemperature. Magana and Quintanilla (2014) [29] investigated the uniqueness and analyticity of solutions in micropolar thermoviscoelasticity. The fundamental solution of the system of equations of steady vibrations was constructed by means of elementary functions and its basic properties were established by Svanadze (2014) [30].

In the present investigation the reflection of plane wave in heat conducting transversely isotropic micropolar viscoelastic half space has been discussed. The amplitude ratios of various waves corresponding to reflected waves are obtained numerically when different waves are incident. The effect of viscosity on the amplitude ratios are shown graphically for specific model. Some particular results are also deduced.

2. Basic equations

The basic equations in a homogeneous anisotropic micropolar viscothermoelastic solid in the absence of body forces, body couples, and heat sources are given by

(a) The constitutive relations.

$$t_{kl} = \overline{A}_{klmn} E_{mn} + \overline{G}_{klmn} \Psi_{mn} - \beta_{kl}(1 + \tau_1 \frac{\partial}{\partial t})T, \tag{1}$$

$$m_{kl} = \overline{B}_{lkmn} E_{mn} + \overline{G}_{mnlk} \Psi_{mn}, \tag{2}$$

$$q_k = K_{kl} T_{,k}, \tag{3}$$

for Lord and Shulman (L-S) theory

$$\rho\eta T_0 = \rho C^* T + \beta_{\mathrm{kl}} T_0 u_{\mathrm{r,r}}, \quad (q_{\mathrm{k,k}} + \tau_0 q_{\mathrm{k,k}}) = K_{\mathrm{kl}} T_{,\mathrm{kk}}, \tag{4}$$

for Green and Lindsay(G-L) theory

$$\rho\eta T_0 = \rho C^* (T + \tau_0 \dot{T}) + \beta_{\mathrm{kl}} T_0 u_{\mathrm{r,r}}, \qquad q_{\mathrm{k,k}} = K_{\mathrm{kl}} T_{,\mathrm{kk}}. \tag{5}$$

The deformation and wryness tensor are defined by the following:

$$E_{\mathrm{kl}} = u_{\mathrm{l,k}} + \varepsilon_{\mathrm{lkm}} \varphi_{\mathrm{m}}, \qquad \Psi_{\mathrm{kl}} = \varphi_{\mathrm{k,l}}. \tag{6}$$

(b) Balance laws.

$$t_{kl,k} = \rho \ddot{u}_l, \tag{7}$$

$$m_{kl,k} + \varepsilon_{lmn} t_{mn} = \rho j \ddot{\phi}_l, \qquad i, j, k = 1,2,3, \tag{8}$$

$$q_{k,k} = \rho T_0 \dot{\eta}, \tag{9}$$

Assuming the viscoelastic nature of the material is described by the Voigt (1887) [1] model of linear elasticity, we replace the micropolar elastic constants $\overline{A}_{ijkl}$, $\overline{\beta}_{ijkl}$,$\overline{G}_{ijkl}$ by their complex moduli as

$$\overline{A}_{\mathrm{ijkl}} = A_{\mathrm{ijkl}} + A^{\upsilon}{}_{\mathrm{ijkl}} \frac{\partial}{\partial t}, \quad \overline{B}_{\mathrm{ijkl}} = \beta_{\mathrm{ijkl}} + \beta^{\upsilon}{}_{\mathrm{ijkl}} \frac{\partial}{\partial t}, \quad \overline{G}_{\mathrm{ijkl}} = G_{\mathrm{ijkl}} + G^{\upsilon}{}_{\mathrm{ijkl}} \frac{\partial}{\partial t}, \tag{10}$$

where $t_{\mathrm{kl}}, m_{\mathrm{kl}}, K_{\mathrm{kl}}$ are the stress tensor, couple stress tensor and thermal conductivity tensor, respectively; q_k is the heat flux vector; η is the entropy; T is the absolute temperature; C^* is the specific heat at constant strain; τ_0, τ_1 are thermal relaxation times; ρ is the bulk mass density; j is the microinertia; u_l, ϕ_k are components of displacement vector and microrotation vector; β_{kl} is thermal elastic coupling tensor; $\overline{A}_{\mathrm{klmn}}, \overline{G}_{\mathrm{klmn}}, \overline{B}_{\mathrm{lkmn}}$ are characteristic constants of material, where $\overline{A}_{\mathrm{klmn}}, \overline{B}_{\mathrm{lkmn}}$ satisfies the symmetric properties

$$\overline{A}_{klmn} = \overline{A}_{mnkl}, \quad \overline{B}_{mnlk} = \overline{B}_{lkmn}, \tag{11}$$

and $\beta_{kl} = \beta_{lk}$, and $K_{kl} = K_{lk}$. Tensor $\overline{G}_{klmn}$ does not possess this property; it forms a pseudo-tensor, inversion of the coordinate system changing its sign. In a centrosymmetric body, all components of $\overline{G}_{\mathrm{klmn}}$ vanish.

For Lord-Shulman (1967) [31] theory $\tau_1 = 0, \eta_0 = 1$; for Green-Lindsay (1972) [32] theory, $\tau_1 > 0, \eta_0 = 0$ and for coupled thermoelasticity theory, $\tau_0 = \tau_1 = 0, \eta_0 = 0$. The thermal relaxation times τ_0 and τ_1 satisfy the inequality $\tau_0 \geq \tau_1 \geq 0$ for G-L theory only. However, it

has been proved by Strunin (2001) [33] that the inequalities are not mandatory for τ_0 and τ_1 to follow.

We introduce the dimensionless quantities as

$$x_i' = \frac{\omega^*}{c_1} x_i, \qquad u_i' = \frac{\omega^*}{c_1} u_i, \qquad \varphi'_2 = \frac{\bar{A}_{55}}{K_1}\varphi_2, \quad m'_{ij} = \frac{c_1}{\bar{B}_{56}\omega^*} m_{ij}, \qquad t'_{ij} = \left(\frac{t_{ij}}{\bar{A}_{11}}\right), \quad \tau_0' = \omega^*\tau_0,$$

$$t' = \omega^* t, \qquad T' = \frac{T}{T_0}, \qquad \omega^{*2} = \frac{X}{\rho j}, \qquad c_1^2 = \frac{\bar{A}_{11}}{\rho}, \qquad \tau_0' = \omega^*\tau_0. \tag{12}$$

where ω^* is the characteristic frequency of the material.

3. Formulation and solution of the problem

Following Slaughter (2002) [34], we use the appropriate transformation on the system of equations (1)-(3) and (4)-(6) to deduce the equations for transversely isotropic micropolar viscothermoelastic medium initially in an undeformed state and at uniform temperature T_0. We take the origin of the coordinate system on the top plane surface and x_3-axis is pointing normally into the half space, which is thus represented by $x_3 \geq 0$.We consider plane waves in a plane such that all particles on a line parallel to $x_2 - axis$ are equally displaced , so all partial derivatives with respected the variable x_2 would be zero.

For two dimensional problem, we take $\vec{u} = (u_1, 0, u_3)$, $\vec{\phi} = (0, \phi_2, 0)$ so that

$$\bar{A}_{11}\frac{\partial^2 u_1}{\partial x_1^2} + (\bar{A}_{13} + \bar{A}_{56})\frac{\partial^2 u_3}{\partial x_1 \partial x_3} + \bar{A}_{55}\frac{\partial^2 u_1}{\partial x_3^2} + K_1\frac{\partial \phi_2}{\partial x_3} - \beta_1(1+\tau_1\frac{\partial}{\partial t})\frac{\partial T}{\partial x_1} = \rho\frac{\partial^2 u_1}{\partial t^2}, \tag{13}$$

$$\bar{A}_{66}\frac{\partial^2 u_3}{\partial x_1^2} + (\bar{A}_{13} + \bar{A}_{56})\frac{\partial^2 u_1}{\partial x_1 \partial x_3} + \bar{A}_{33}\frac{\partial^2 u_3}{\partial x_3^2} + K_2\frac{\partial \phi_2}{\partial x_1} - \beta_3(1+\tau_1\frac{\partial}{\partial t})\frac{\partial T}{\partial x_3} = \rho\frac{\partial^2 u_3}{\partial t^2}, \tag{14}$$

$$\beta_{77}\frac{\partial^2 \phi_2}{\partial x_1^2} + \beta_{66}\frac{\partial^2 \phi_2}{\partial x_3^2} - \chi\phi_2 + K_1\frac{\partial u_1}{\partial x_3} + K_2\frac{\partial u_3}{\partial x_1} = \rho j\frac{\partial^2 \phi_2}{\partial t^2}, \tag{15}$$

$$K_1^*\frac{\partial^2 T}{\partial x_1^2} + K_3^*\frac{\partial^2 T}{\partial x_3^2} = \rho c^*\left(\frac{\partial}{\partial t} + \tau_0\frac{\partial^2}{\partial t^2}\right)T + T_0\left(\frac{\partial}{\partial t} + n_0\tau_0\frac{\partial^2}{\partial t^2}\right)\left(\beta_1\frac{\partial u_1}{\partial x_1} + \beta_3\frac{\partial u_2}{\partial x_2}\right), \tag{16}$$

$$t_{33} = \bar{A}_{13}\frac{\partial u_1}{\partial x_1} + \bar{A}_{33}\frac{\partial u_3}{\partial x_3} - \beta_3(1+\tau_1\frac{\partial}{\partial t})T, \tag{17}$$

$$t_{31} = \bar{A}_{65}\frac{\partial u_3}{\partial x_1} + K_1\phi_2 + \bar{A}_{55}\frac{\partial u_1}{\partial x_3}, \qquad m_{32} = \bar{A}_{66}\frac{\partial \phi_2}{\partial x_3}, \tag{18, 19}$$

where $\beta_1 = \bar{A}_{11}\alpha_1 + \bar{A}_{13}\alpha_3$, $\beta_3 = \bar{A}_{31}\alpha_1 + \bar{A}_{33}\alpha_3$, $K_1 = \bar{A}_{56} - \bar{A}_{55}$, $K_2 = \bar{A}_{66} - \bar{A}_{56}$, $X = K_2 - K_1$, α_1, α_3 are the coefficients of linear thermal expansion, we have used the notations $11 \to 1$, $33 \to 3$, $12 \to 7$, $13 \to 6$, $23 \to 5$ for the material constants.

We take plane-wave solution as

$$(u_1, u_3, \varphi_2, T) = (\tilde{u}_1, \tilde{u}_3, \tilde{\varphi}_2, \tilde{T})\, e^{i\xi(x_1 p_1 + p_3 x_3 - ct)}. \tag{20}$$

Substituting the values of u_1, u_3, φ_2 and T from equation (20) in the equations (13)-(16) and with the aid of (12) and after some simplification we obtain

$$c^8 + A_1c^6 + A_2c^4 + A_3c^2 + A_4 = 0, \tag{21}$$

where $A_1 = \frac{\omega^2 f_1 + f_6}{a_4\omega^2 - a_5}$, $A_2 = \frac{f_3\omega^4 + (f_2 + f_4)\omega^2 + f_4}{a_4\omega^4 - a_5\omega^2}$, $A_3 = \frac{f_5\omega^2 + f_7}{a_4\omega^2 - a_5}$, $A_4 = \frac{f_8\omega^2}{a_4\omega^2 - a_5}$,

$f_1 = a_1 - a_2' - a_4b_1$, $f_2 = a_8 - a_2 - a_4b_1 + a_{17}b_{14} + a_{12}b_{15} - b_1a_5$, $f_3 = a_6' - a_1 - a_3 + a_2'b_1 + a_{12}'b_{10}$,

$f_4 = a_6 + b_1a_2 + b_{10}(a_{12} - a_{13}') + b_{14}(a_{15} - a_{18} + a_{15}') - b_{15}a_{18}$, $f_5 = a_7 + a_3b_1 + a_9b_{10} - b_1a_6'$,

$f_6 = a_5b_1 - b_{15}a_{22} - a_4b_1$, $f_7 = a_{14}b_{14} + a_{20}b_{15} - a_6b_1 - b_{10}a_{10}$, $f_8 = -a_7b_1 - a_{11}b_{10}$,

$f_9 = a_{19}b_{15} - b_1a_8 - a_{13}b_{10}$, $a_1 = d_7b_8d_{12}$, $a_2 = d_7(b_8d_{11} + d_6d_9) + b_4b_7d_{12}$, $a_2' = b_2b_9d_{12}$,

$a_3 = b_8(b_6d_7 + b_2d_{12})$, $a_4 = d_{12}d_7b_9$, $a_5 = d_7d_{11}b_9$, $a_6 = b_4b_6b_7 + b_8(b_2d_{11} - b_3b_5)$, $a_6' = b_2b_6b_9$,

$a_7 = b_2b_6b_8$, $a_8 = b_9(b_2d_{11} - b_3b_5)$, $a_9 = b_9b_{11}d_{12}$, $a_{10} = b_{11}(b_8d_{11} + b_6d_9) + b_5b_8b_{11} - b_6b_7b_{13}$,

$a_{11} = b_6b_8b_{11}$, $a_{12} = -b_7b_{13}d_{12}$, $a_{12}' = b_9b_{11}d_{12}$, $a_{13} = b_7b_{13}d_{11}$, $a_{13}' = b_9(b_{11}d_{12} + b_5b_{12})$,

$a_{14} = b_8(b_1b_3 + b_2b_{12})$, $a_{15} = b_7(b_4b_{12} - b_3b_{13})$, $a_{15}' = b_9(b_1b_3 + b_2b_{12})$, $a_{16} = b_8b_{12}d_7$, $a_{17} = -b_9b_{12}d_7$,

$a_{18} = d_{12}(b_4b_{11} + b_2b_{13})$, $a_{19} = d_{11}(b_{14}b_4 + b_2b_{13}) - b_6b_{13}d_7 + b_5(b_4b_{11} - b_3b_{13})$, $a_{20} = b_6(b_4b_{11} + b_2b_{13})$,

$a_{21} = b_{13}d_{12}d_7$, $a_{22} = b_{13}d_7d_{11}$, $b_1 = d_1p_3^2 + p_1^2$, $b_2 = d_5p_3^2 + p_1^2d_4$, $b_3 = \mathrm{i}p_1d_{10}$,

$b_4 = p_3\omega\varepsilon_2(1 - \mathrm{i}\omega\tau_1)$ $b_5 = \mathrm{i}p_1d_6$, $b_6 = d_7p_3^2 + p_1^2d_8$, $b_7 = -\mathrm{i}p_3d_{14}(1 - \mathrm{i}\omega\tau_1)$, $b_8 = p_3^2 + \bar{k}p_1^2$,

$b_9 = -\mathrm{i}\varepsilon_1(1/\omega - \mathrm{i}\tau_0)$, $b_{10} = p_1p_3d_2$, $b_{11} = -p_1p_3d_5$, $b_{12} = \mathrm{i}p_3d_9$, $b_{13} = p_3\omega\varepsilon_2p_1\bar{\beta}(1 - \mathrm{i}\omega\tau_1)$,

$b_{14} = \mathrm{i}p_3d_3$, $b_{15} = -\mathrm{i}p_1d_3(1 - \mathrm{i}\omega\tau_1)$, $d_1 = \frac{\bar{A}_{55}}{\bar{A}_{11}}$, $d_2 = \frac{\bar{A}_{13} + \bar{A}_{56}}{\bar{A}_{11}}$, $d_3 = \frac{K_1^2}{\bar{A}_{11}\bar{A}_{55}}$, $d_4 = \frac{\bar{A}_{66}}{\bar{A}_{11}}$, $d_5 = \frac{\bar{A}_{33}}{\bar{A}_{11}}$,

$d_6 = \frac{K_1K_2}{\bar{A}_{55}\bar{A}_{11}}$, $d_7 = \frac{\bar{B}_{66}}{\rho jc_1^2}$, $d_8 = \frac{\bar{B}_{77}}{\rho jc_1^2}$, $d_9 = \frac{X}{\rho j\omega^{*2}}$, $d_{10} = \frac{\bar{A}_{55}}{\rho j\omega^{*2}}$, $d_{11} = \frac{K_2}{K_1}d_{10}$, $d_{13} = \frac{\beta_3T_0}{\bar{A}_{11}}$, $d_{18} = \frac{\bar{A}_{13}}{\bar{A}_{11}}$,

$d_{14} = \frac{\beta_1T_0}{\bar{A}_{11}}$, $d_{15} = \frac{K_1^*}{\bar{A}_{55}}$, $d_{16} = \frac{\bar{A}_{56}}{\bar{A}_{11}}$, $\bar{\beta} = \frac{\beta_1}{\beta_3}$, $\varepsilon_1 = \frac{\rho C^*c_1^2}{K_3^*\omega^*}$, $\varepsilon_2 = \frac{\beta_3c_1^2}{K_3^*\omega^*}$, $\bar{k} = \frac{K_1^*}{K_3^*}$, $\tag{22}$

where $\vec{p}(p_1, 0, p_3)$ denotes the unit propagation vector.

The characteristic equation (21) having the complex coefficients yields the four complex roots. The complex phase velocities c_i, $(i = 1,2,3,4)$ of the quasi-waves will be varying with the direction of phase propagation. We take the complex velocity $c_i = c_R + ic_I$ and define the wave propagation velocity $V_i = \frac{c_R^2 + c_I^2}{c_R}$ and the attenuation quality factor $Q^{-1} = -2c_I / c_R$. These waves become homogeneous wave if they have same direction of wave propagation and attenuation vector of these waves. These waves are called quasi-waves because polarization may not be along the dynamic axes. The wave velocity V_i, $(i = 1,2,3,4)$ are

named as quasi-longitudinal displacement (qLD) wave, quasi transverse microrotational (qTM), quasi-transverse displacement (qTD) wave and quasi-thermal wave (qT) that are propagating with the descending phase velocities respectively.

4. Reflection at the free surface

Let us consider free surface $x_3 = 0$ for transversely isotropic micropolar viscothermoelastic half-space occupying the region $x_3 > 0$ (Fig. 1).

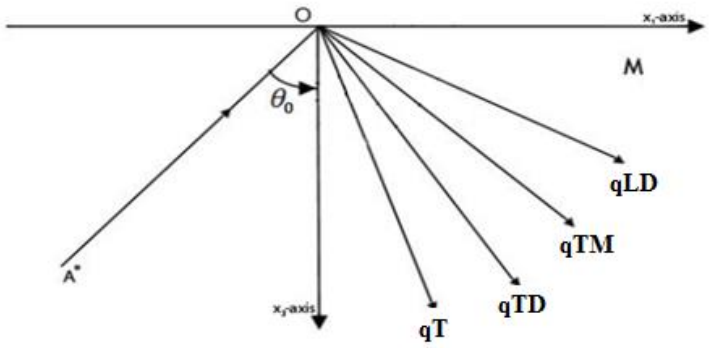

Fig. 1. Geometry of the problem.

We assume qLD or qTD or qTM or qT wave is incident at the interface and each Incident wave will generate reflected qLD, qTD, qTM and qT waves in free surface. The total displacement, microrotations and temperature distributions are

$$u_1 = \sum_{j=1}^{8} A_j e^{t\omega[t-(x_1 \sin e_j - x_3 \cos e_j)/c_j]} \quad , \quad u_3 = \sum_{j=1}^{8} B_j e^{t\omega[t-(x_1 \sin e_j - x_3 \cos e_j)/c_j]} \, ,$$

$$\varphi_2 = \sum_{j=1}^{8} C_j e^{t\omega[t-(x_1 \sin e_j - x_3 \cos e_j)/c_j]} \quad , \quad T = \sum_{j=1}^{8} D_j e^{t\omega[t-(x_1 \sin e_j - x_3 \cos e_j)/c_j]} \, , \qquad (j = 1,.....,8) \, , \quad (23)$$

where ω is the angular frequency. The subscripts 1,…., 4 denote the quantities corresponding to incident qLD, qTD, qTM and qT wave, respectively, whereas the subscripts 5,… 8, respectively, denote the corresponding reflected wave and

$B_j = \frac{A_{1i}}{A_i} A_j \quad , C_j = \frac{A_{2i}}{A_i} A_j \quad , D_j = \frac{A_{3i}}{A_i} A_j \, , \quad (j = 1,.....,8)$, where A_i, A_{1i}, A_{2i}, A_{3i} are obtained as

$$A_i = -\xi b_4 [(\omega^2 - d_{11} - b_6 \xi^2)(\xi b_7)] + (b_9 + b_8 \xi^2)[(d_7 \omega^2 - b_2 \xi^2)(\omega^2 - d_{11} - b_6 \xi^2) - \xi^2 b_3 b_5 \, ,$$

$$A_{1i} = -\xi b_{13} [(\omega^2 - d_{11} - b_6 \xi^2)(\xi b_7) + (b_9 + b_8 \xi^2)[(b_{11} \xi^2)(\omega^2 - d_{11} - b_6 \xi^2) - \xi^2 b_5 b_{12}] \, ,$$

$$A_{2i} = \xi^3 b_7 [b_4 b_{12} - b_{13} b_3] + (b_9 + b_8 \xi^2)[\xi^3 b_3 b_{11} - \xi b_{12} (d_7 \omega^2 - b_2 \xi^2)] \, ,$$

$$A_{3i} = = \xi^3 b_5 [b_{12} b_4 - b_{13} b_3] - (\omega^2 - d_{11} - b_6 \xi^2)[\xi^3 b_{11} b_4 - \xi b_{13} (d_7 \omega^2 - b_2 \xi^2)] . \qquad (24)$$

The expressions for a_i, $i = 1,2,.....15$ are obtained from the expressions for a_i, $i = 1,2,.....15$ given in equation (22) on substituting the values for p_1 and p_2.

For incident qLD wave $p_1 = \sin e_1$, $p_3 = -\cos e_1$; for incident qTD wave $p_1 = \sin e_2$, $p_3 = -\cos e_2$; for incident qTM wave $p_1 = \sin e_3$, $p_3 = -\cos e_3$; for incident qT wave

$p_1 = \sin e_4$, $p_3 = -\cos e_4$; for reflected qLD wave $p_1 = \sin e_5$, $p_3 = \cos e_5$; for reflected qTD wave $p_1 = \sin e_6$, $p_3 = \cos e_6$; for reflected qTM wave $p_1 = \sin e_7$, $p_3 = \cos e_7$; for reflected qT wave $p_1 = \sin e_8$, $p_3 = \cos e_8$.

5. Boundary conditions

Mechanical condition:

Mechanical conditions are the vanishing of the normal stress, tangential stress, tangential couple stress components and these can be written mathematically as

$$t_{33} = t_{31} = m_{32} = 0, \text{ at } x_3 = 0 \ . \tag{25}$$

Thermal condition:

$$\frac{\partial T}{\partial x_2} + hT = 0 \ , \tag{26}$$

where $h \to 0$ corresponds to thermally insulated boundaries and $h \to \infty$ refers to isothermal boundaries.

The boundary conditions given by equations (25) to (26) can be satisfied for all values of x_1 and *t*, therefore we have

$$E_1(x_1,0,t) = E_2(x_1,0,t) = \ldots\ldots\ldots\ldots\ldots\ldots\ldots\ldots\ldots\ldots = E_8(x_1,0,t) \tag{27}$$

From the equations (23) and (27), we have

$$\frac{\sin e_1}{c_1} = \frac{\sin e_2}{c_2} = \ldots\ldots\ldots\ldots\ldots\ldots = \frac{\sin e_7}{c_7} = \frac{\sin e_8}{c_8} = \frac{1}{c} \ , \tag{28}$$

which corresponds to the Snell's law and

$$\xi_1 c_1 = \xi_2 c_2 = \ldots\ldots\ldots\ldots\ldots\ldots\ldots\ldots\ldots\ldots = \xi_8 c_8 = \omega \, , \tag{29}$$

where $e_1 = e_5$, $e_2 = e_6$, $e_3 = e_7$ and $e_4 = e_8$, and $c_1 = c_5$, $c_2 = c_6$, $c_3 = c_7$ and $c_4 = c_8$. Substituting the values of u_1, u_3, ϕ_2, *T* from (23) in boundary conditions (25)-(26) and with the help of equations (17) - (19), (28), and (29) yield

$$\sum_{j=1}^{8} A_{ij} A_j = 0 \quad , \quad (i = 1,\ldots\ldots\ldots\ldots,4) \, , \tag{30}$$

where $A_{1\mathrm{j}} = -d_{18}F_1 + r_{\mathrm{j}} d_5 F_2 - t_{\mathrm{j}} F_3 \quad (\mathrm{j} = 1,\ldots\ldots,4)$; $A_{1\mathrm{j}} = -d_{18}F_1 - r_{\mathrm{j}} d_5 F_2 - t_{\mathrm{j}} F_3 \quad (\mathrm{j} = 5,\ldots\ldots,8)$;
$A_{2\mathrm{j}} = d_1 F_2 - r_{\mathrm{j}} d_{16} F_1 + s_{\mathrm{j}} d_{17} \quad (\mathrm{j} = 1,\ldots\ldots,4)$; $A_{2\mathrm{j}} = -d_1 F_2 - r_{\mathrm{j}} d_{16} F_1 + s_{\mathrm{j}} d_{17} \quad (\mathrm{j} = 5,\ldots\ldots,8)$;
$A_{3\mathrm{j}} = d_{15} s_{\mathrm{j}} F_2$, $A_{4\mathrm{j}} = t_{\mathrm{j}} F_2 \ (\mathrm{j} = 1,\ldots\ldots,4)$; $A_{3\mathrm{j}} = -d_{15} s_{\mathrm{j}} F_2$, $A_{4\mathrm{j}} = -t_{\mathrm{j}} F_2 \ (\mathrm{j} = 5,\ldots\ldots,8)$,

where $F_1 = \dfrac{\sin e_{\mathrm{j}}}{c_{\mathrm{j}}}$, $F_2 = \dfrac{\cos e_{\mathrm{j}}}{c_{\mathrm{j}}}$, $F_3 = d_{13}(1 + \tau_1 \omega)$.

For incidence of qLD wave $A_2 = A_3 = A_4 = 0$. We obtain a system of four non-homogeneous equations in four unknowns which on simplification yield

$$Z_{\mathrm{i}} = \frac{A_{\mathrm{i}+4}}{A_1} = \frac{\Delta_{\mathrm{i}}^1}{\Delta} \qquad (\mathrm{i} = 1,\ldots\ldots\ldots\ldots,4) \, , \tag{31}$$

For incidence of qTD wave $A_1 = A_3 = A_4 = 0$ and we have

$$Z_i = \frac{A_{1+4}}{A_2} = \frac{\Delta_i^2}{\Delta} \qquad (i = 1,.....,4), \tag{32}$$

For incidence of qTM wave $A_1 = A_2 = A_4 = 0$ and we obtain

$$Z_i = \frac{A_{1+4}}{A_3} = \frac{\Delta_i^3}{\Delta} \qquad (i = 1,.....,4). \tag{33}$$

For incidence of qT wave $A_1 = A_2 = A_3 = 0$ and which yield

$$Z_i = \frac{A_{1+4}}{A_4} = \frac{\Delta_i^4}{\Delta} \qquad (i = 1,.....,4), \tag{34}$$

where $\Delta = |A_{ii+4}|_{4\times4}$ and $\Delta_i^p\ (i = 1,2.....,4)\ \ (p = 1,.....,4)$ are obtained by replacing , respectively, the 1st, 2nd, ……., 4th columns of Δ by $\left[-A_{1p}\ ,-A_{2p}\ ,-A_{3p}\ ,-A_{4p}\right]^T$.

6. Numerical results and discussion

To illustrate the numerical results graphically, the value for relevant parameters for transversely isotropic micropolar viscothermoelastic medium are taken as

$A_{11} = 17.8\times10^{10}\,\mathrm{Nm}^{-2}$, $A_{33} = 1.843\times10^{10}\,\mathrm{Nm}^{-2}$, $A_{55} = 4.357\times10^{10}\,\mathrm{Nm}^{-2}$, $A_{66} = 4.42\times10^{10}\,\mathrm{Nm}^{-2}$, $A_{13} = 7.59\times10^{10}\,\mathrm{Nm}^{-2}$, $A_{56} = 4.357\times10^{10}\,\mathrm{Nm}^{-2}$, $B_{77} = 2.63\times10^{9}\,\mathrm{N}$, $B_{66} = 5.648\times10^{9}\,\mathrm{N}$, $\rho = 1.74\,\mathrm{kg/m}^3$, $T_0 = 2.98\mathrm{K}$, $C^* = 1.04\,\mathrm{Cal/K}$, $K_1^* = 1.7\,\mathrm{Cal/K}$, $j = 0.02\,\mathrm{m}^2$, $\tau_0 = 0.4\mathrm{s}$, $\tau_1 = 0.8\mathrm{s}$.

For a particular model of heat conducting transversely isotropic micropolar viscothermoelastic solid half space we take $\bar{\chi}_i = \chi(1 - iR_i)$, where $\chi = A_{11},\ A_{13},\ A_{33},\ A_{55},\ A_{56},\ A_{66},\ B_{66},\ B_{77}$ and $R_1 = 10.05,\ R_2 = 2.6,\ R_3 = 3.2,\ R_4 = 7.9,\ R_5 = 7.03,\ R_6 = 2.01,\ R_7 = 1.7,\ R_8 = 5.8$.

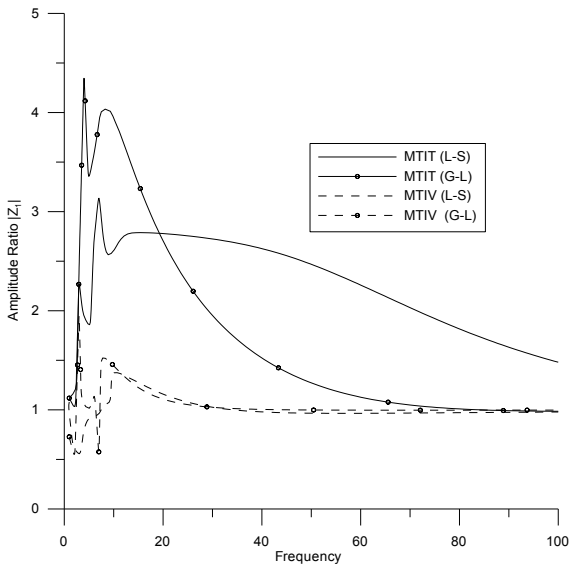

Fig. 2. Amplitude Ratio $|Z_1|$ when qLD wave is incident.

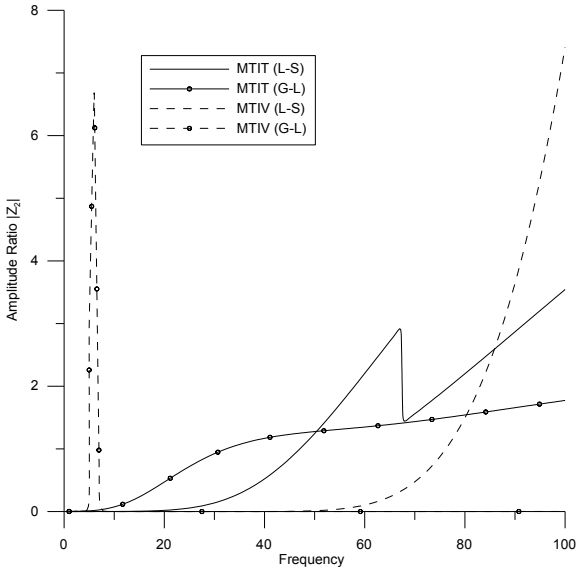

Fig. 3. Amplitude Ratio $|Z_2|$ when qLD wave is incident.

Figures 2-5 show the variation of amplitude ratio $|Z_i|$, $(i=1,2,3,4)$ with respect to frequency when qLD wave is incident. Figures 6-9 show the variation of amplitude ratio $|Z_i|$, $(i=1,2,3,4)$ with respect to frequency when qTM wave is incident. Figures 10-13 show the variation of amplitude ratio $|Z_i|$, $(i=1,2,3,4)$ with respect to frequency when qTD wave is incident.

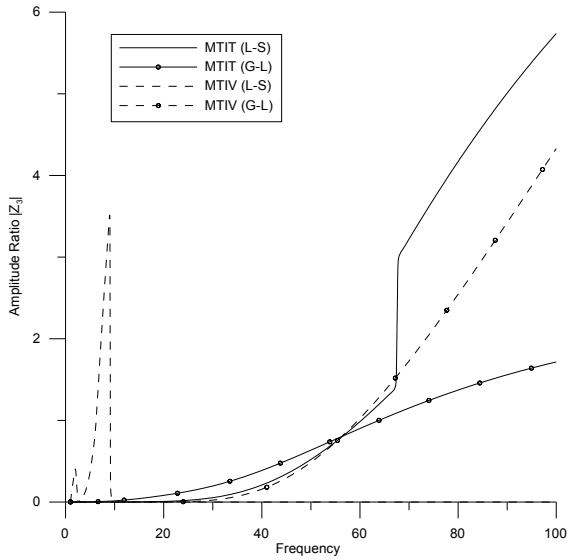

Fig. 4. Amplitude Ratio $|Z_3|$ when qLD wave is incident.

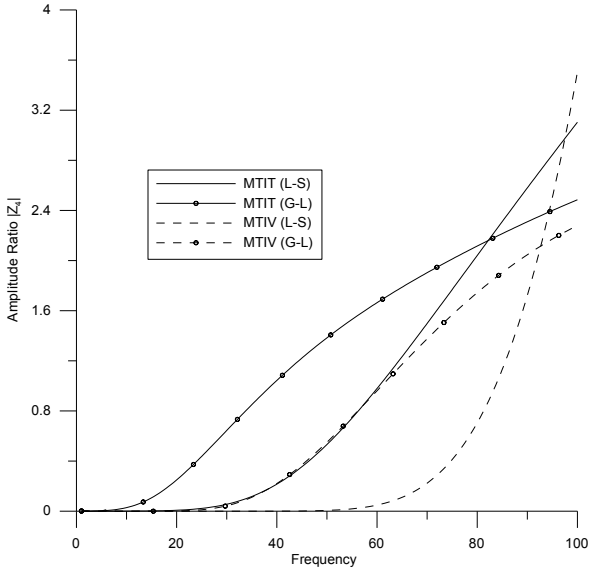

Fig. 5. Amplitude Ratio $|Z_4|$ when qLD wave is incident.

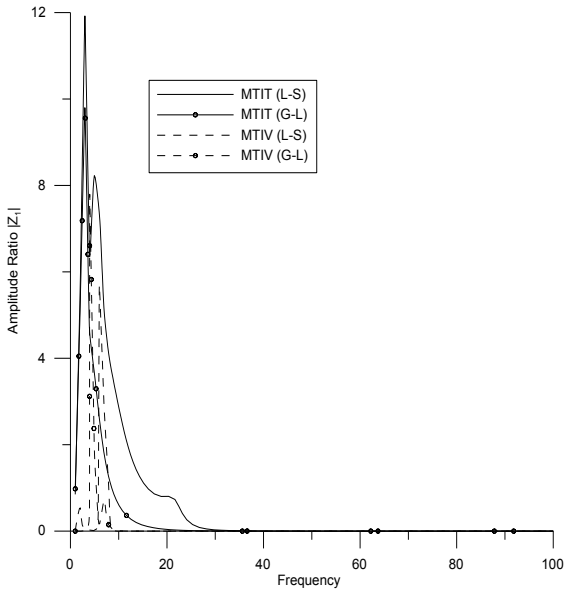

Fig. 6. Amplitude Ratio $|Z_1|$ when qTM wave is incident.

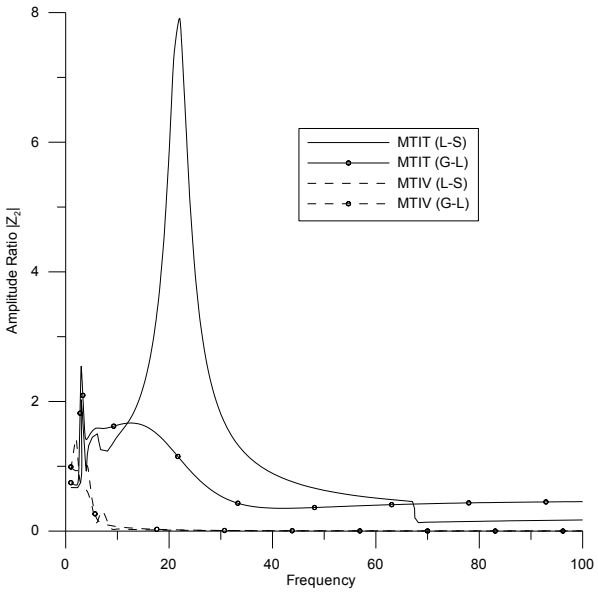

Fig. 7. Amplitude Ratio $|Z_2|$ when qTM wave is incident.

Figures 13-17 show the variation of amplitude ratio $|Z_i|$, $(i=1,2,3,4)$ with respect to frequency when qT wave is incident. In all figures, effect of viscosity along with relaxation times has been shown for transversely isotropic micropolar thermoelastic half space and transversely isotropic micropolar viscothermoelastic half space. In case of L-S theory, the solid lines corresponds to transversely isotropic micropolar thermoelastic half space is MTIT(L-S) and dotted line corresponds to transversely isotropic micropolar

viscothermoelastic half space is MTIV(L-S). In case of G-L theory the solid lines with node corresponds to transversely isotropic micropolar thermoelastic half space is MTIT(G-L) and dotted line with node corresponds to transversely isotropic micropolar viscothermoelastic half space is MTIV(G-L).

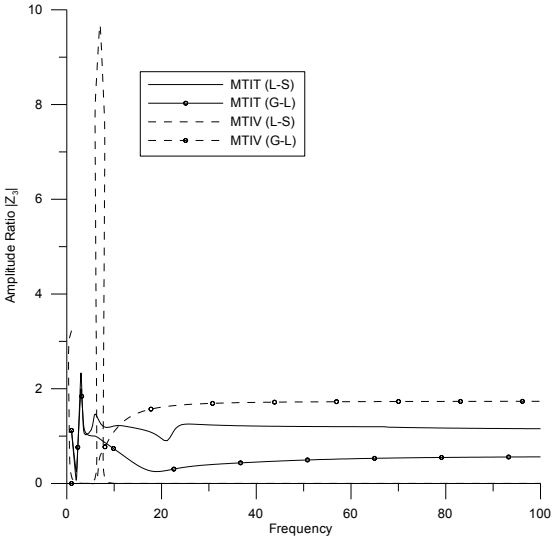

Fig. 8. Amplitude Ratio $|Z_3|$ when qTM wave is incident.

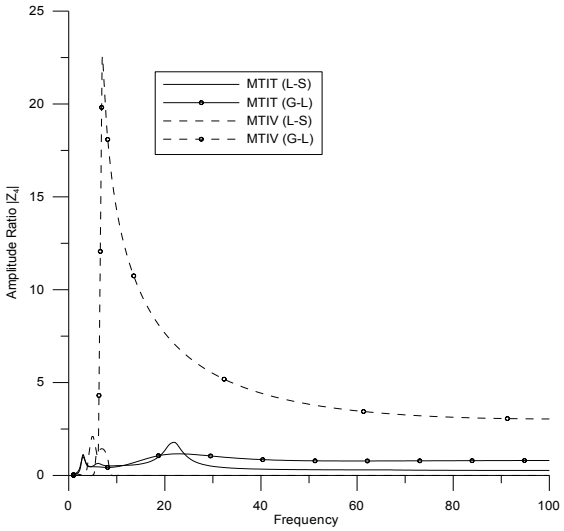

Fig. 9. Amplitude Ratio $|Z_4|$ when qTM wave is incident.

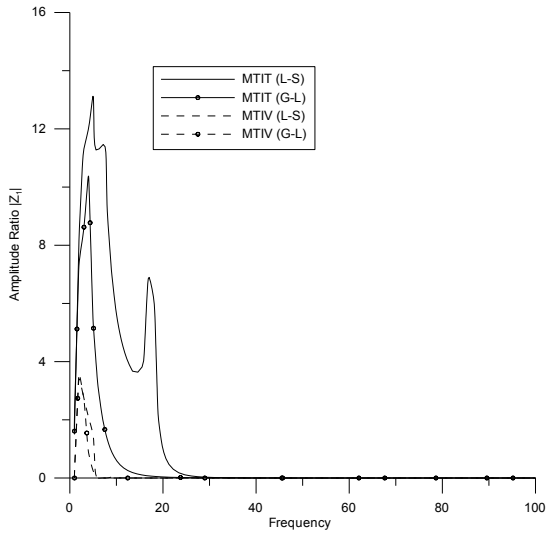

Fig. 10. Amplitude Ratio $|Z_1|$ when qTD wave is incident.

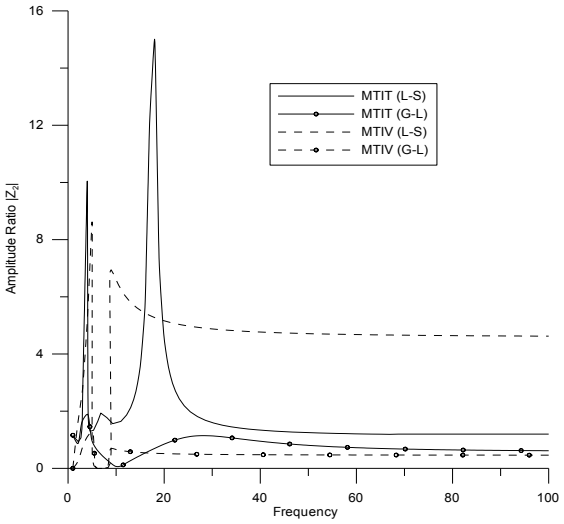

Fig. 11. Amplitude Ratio $|Z_2|$ when qTD wave is incident.

When qLD wave is incident. Figure 2 shows the variation of amplitude ratio $|Z_i|$ with respect to frequency when qLD wave is incident. The values of amplitude ratio $|Z_1|$ is more for MTIT(L-S) as compared to MTIV(L-S) for $0 \le \omega \le 80$ due to viscous effect and finally becomes dispersonless. The values of amplitude ratio $|Z_1|$ increase monotonically for MTIT(G-L) in $0 \le \omega \le 10$ and decrease gradually for $11 \le \omega \le 100$, for MTIV(G-L), the values oscillate for the region $0 \le \omega \le 10$ and as $\omega \ge 10$, the values increase.

In Figure 3, the value of amplitude ratio $|Z_2|$ for MTIT(L-S) oscillates initially and then increase linearly, and for MTIV(L-S) the value increase slowly as ω increases. For

MTIV(G-L), the value of $|Z_2|$ initially oscillates and become stationary as ω increases, whereas for MTIT(G-L) the value initially oscillates, increases instantaneously remain stationary as ω goes on increasing.

In Figure 4 the value of amplitude ratio $|Z_3|$ oscillates for MTIV(L-S) with initial values of ω and then remain stationary. The value of $|Z_3|$ for MTIT(L-S), MTIT(G-L), MTIV(G-L) increases monotonically as ω increases except for MTIT(L-S) case in which it has some stationary values at the particular value of ω.

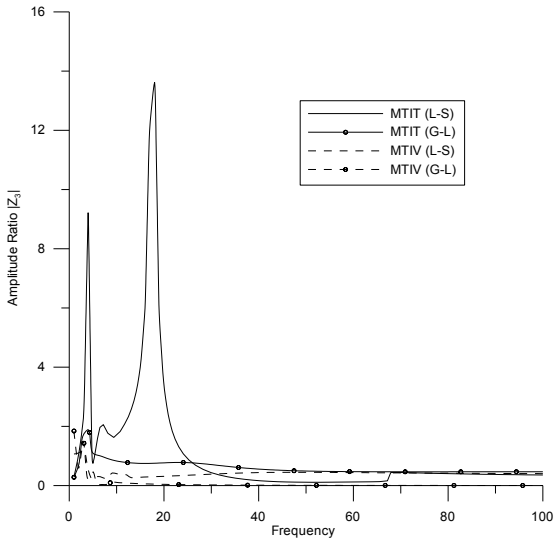

Fig. 12. Amplitude Ratio $|Z_3|$ when qTD wave is incident.

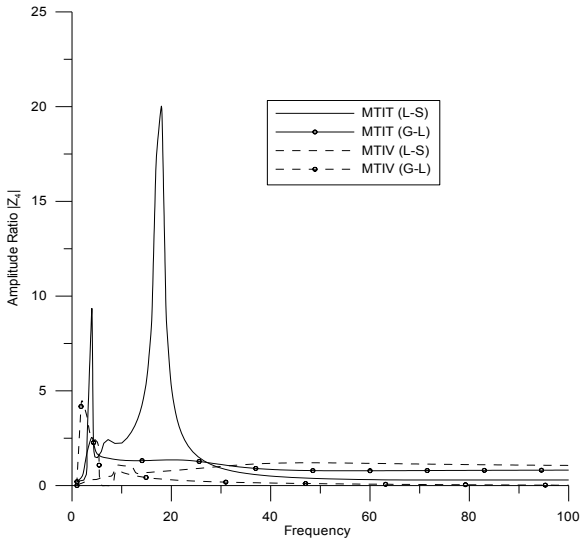

Fig. 13. Amplitude Ratio $|Z_4|$ when qTD wave is incident.

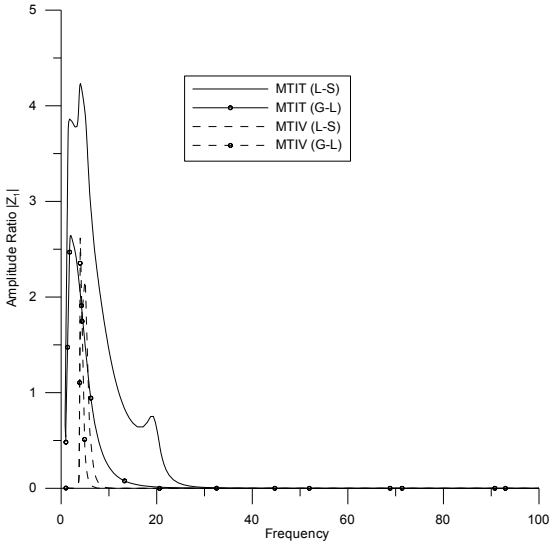

Fig. 14. Amplitude Ratio $|Z_1|$ when qT wave is incident.

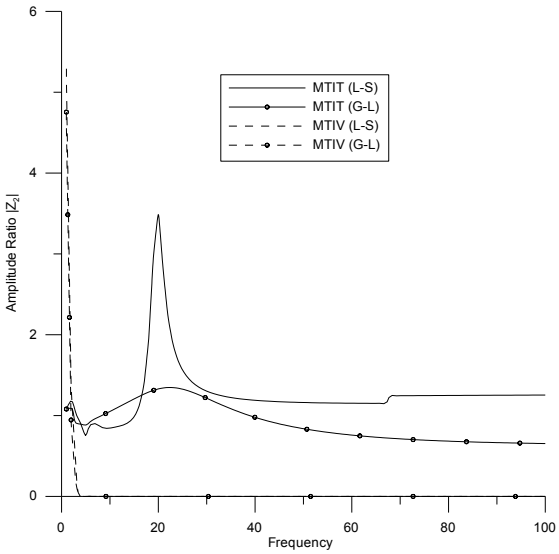

Fig. 15. Amplitude Ratio $|Z_2|$ when qT wave is incident.

In Figure 5 the trend and behavior of variation MTIT(L-S), MTIV(L-S), MTIT(G-L) and MTIV(G-L) are same for all the values of ω. The value of $|Z_4|$ for MTIV(L-S) are smaller in comparison to other cases.

When qTM wave is incident. In Figure 6 the amplitude ratio $|Z_1|$ oscillates for $0 \le \omega \le 10$ and attains peak values for MTIT(G-L) and instantly vanishes for $\omega \ge 25$. For

MTIV (L-S) and MTIV(G-L) the value of $|Z_1|$ oscillates for $0 \le \omega \le 10$ and vanishes for $\omega \ge 10$. Similar behavior is observed for MTIT(L-S) and MTIT(G-L) theories within $20 \le \omega \le 35$ range of frequency.

In Figure 7 the values of amplitude ratio $|Z_2|$ initially oscillates for $0 \le \omega \le 10$ and decreases as ω increases for MTIV (L-S) and MTIV(G-L). For MTIT(L-S) the value of amplitude ratio is maximum for $\omega \le 20$ and in case of MTIT(G-L) , its value slowly decreases and becomes constant near the boundary surface.

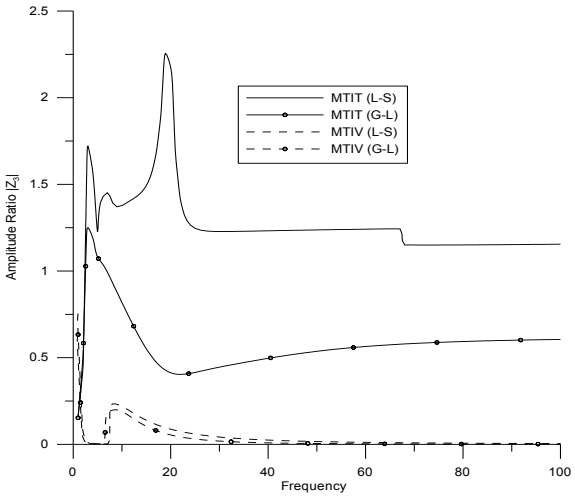

Fig. 16. Amplitude Ratio |Z3| when qT wave is incident.

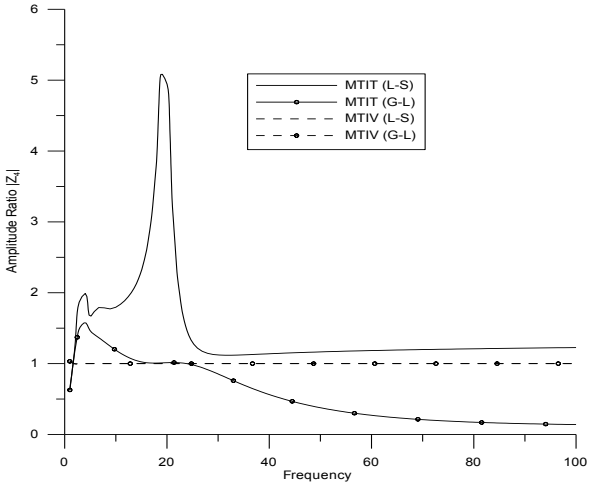

Fig. 17. Amplitude Ratio |Z4| when qT wave is incident.

In Figure 8 the values of $|Z_3|$ oscillates in the interval $0 \le \omega \le 15$ for all the cases attaining the maximum value for MTIV(L-S) and as ω increase further the behavior of $|Z_3|$ is similar and all values of $|Z_3|$ decrease due to viscosity effect for both the theories.

In Figure 9 the values of amplitude ratio $|Z_4|$ near the boundary surface oscillates for both theories and attaining maxima for MTIV(G-L) theory and then decreases as frequency increases. The trend and behavior of $|Z_4|$ as $\omega \ge 30$ is similar as $|Z_3|$ for $\omega \ge 22$.

When qTD wave is incident. In Figure 10 the amplitude ratio $|Z_1|$ oscillates for all the cases when $0 \le \omega \le 20$ and then become stationary for $\omega \ge 20$. The value of $|Z_1|$ decreases due to viscosity effect.

Figure 11 shows the behavior and variation of $|Z_2|$ when qTD wave is incident as that of $|Z_1|$ when qTD wave is incident for $0 \le \omega \le 20$ and as $\omega \ge 20$, the values are stationary for all the cases, but the value of $|Z_2|$ for MTIT(L-S) is more than MTIV(L-S) and the value of $|Z_2|$ for MTIV(G-L) is less than that of MTIT(G-L) showing the viscosity effect.

In Figure 12 the value of amplitude ratio $|Z_3|$ is minimum for MTIV(G-L) as compared to MTIT(G-L) theory and the values of $|Z_3|$ attains maximum for MTIT(L-S) as compared to MTIV(L-S) theory, and then flatten out near the boundaries for both the cases.

In Figure 13 the trend and behavior is similar but the value of $|Z_4|$ is higher for MTIT(L-S) theory due to viscous effect.

When qT wave is incident. In Figure 14 the value of $|Z_1|$ for MTIV(L-S) and MTIV(G-L) are less in comparison to MTIT(L-S) and MTIT(G-L) due to viscosity effect for $0 \le \omega \le 10$ and as $\omega \ge 20$ the values are stationary for all the cases.

In Figure 15 the value of $|Z_2|$ is more for MTIV(L-S) and MTIV(G-L) as compared to MTIT(L-S) and MTIT(G-L) , its value instantaneously increase and decrease as ω increases respectively. The values of MTIT(L-S) and MTIT(G-L) oscillates and become stationary as ω increases .

In Figure 16 the value of $|Z_3|$ for MTIV(L-S) and MTIV(G-L) is opposite to MTIT(L-S) and MTIT(G-L) initially. Also the value of $|Z_3|$ for MTIV(L-S) and MTIV(G-L) decreases as ω increases.

In Figure 17 the value of $|Z_4|$ for MTIV(L-S) and MTIV(G-L) are more than MTIT(L-S) and MTIT(G-L) initially, in the intermediate range of ω the value of $|Z_4|$ are small. As $\omega \ge 25$ the values of $|Z_4|$ for MTIV(L-S) and MTIV(G-L) lie between MTIT(L-S) and MTIT(G-L).

7. Conclusion

In the present investigation, reflections of plane waves in transversely isotropic micropolar thermoelastic solid have been discussed. The trend of variation and behavior of the amplitude ratio $|Z_1|$ is similar for incidence of qLD, qTD, qTM and qT with change in their magnitude values. The value of amplitude ratio $|Z_1|$ for MTIT (L-S) remains more in comparison with MTIT(G-L) for incidence of qTD, qTM and qT, except for qLD, where reverse behavior occurs for the value of $|Z_1|$.

The behavior of $|Z_3|$ is different for all the incident waves, however, the value of amplitude ratio $|Z_4|$ is more in case of G-L theory due to viscosity effect, for the incident of qLD and qTM waves, but for the remaining incident waves the value of amplitude ratio $|Z_4|$ is more for L-S theory.

From the present investigation, it is concluded, that the values of amplitude ratios shows sharp oscillations at initial frequency for incident qT, qTD, qTM as compared to qLD waves. An appreciable effect of viscosity and relaxation time are noticed on amplitude ratios of various reflected waves.

References

[1] W. Voigt // *Abhandlungen der Königlichen Gesellschaft der Wissenschaften zu Göttingen* **34** (1887) 3.
[2] A.C. Eringen // *International Journal of Engineering Science* **5** (1967) 191.
[3] M.F. McCarthy, A.C. Eringen // *International Journal of Engineering Science* **7** (1969) 447.
[4] R. Kumar, M.L. Gogna, L. Debnath // *International Journal of Mathematics and Mathematical Sciences* **13** (1990) 363.
[5] P.K. Biswas, P. R. Sengupta, L. Debnath // *International Journal of Mathematics and Mathematical Sciences* **19** (1996) 815.
[6] S. De Cicco, L. Nappa // *Indian Journal of Engineering, Science, and Technology* **36** (1998) 883.
[7] R. Kumar, B. Singh // *International Journal of Engineering Science* **36** (1998) 119.

[8] R. Kumar, B. Singh // *Indian Journal of Pure and Applied Mathematics* **31** (2000) 287.
[9] B. Singh // *Sadhana - Academy Proceedings of Engineering Sciences* **25(6)** (2000) 589.
[10] R. Kumar // *International Journal of Engineering Science* **38** (2000) 1377.
[11] A.S. El-Karamany // *International Journal of Engineering Science* **40** (2002) 2097.
[12] A.S. El-Karamany // *International Journal of Engineering Science* **42** (2004) 157.
[13] R. Kumar, R. Singh // *International Journal of Applied Mechanics and Engineering* **10** (2005) 227.
[14] I.A. Oathman, Y. Song // *Canadian Journal of Physics* **85(7)** (2007) 797.
[15] R. Kumar, N. Sharma // *International Journal of Manufacturing Science and Technology* **2** (2007) 133.
[16] R. Kumar, G. Partap // *International Journal of Applied Mechanics and Engineering* **13** (2008) 383.
[17] R. Sharma, N. Sharma // *Theoretical and Applied Fracture Mechanics* **50** (2008) 226.
[18] R. Kumar, N. Sharma // *International Journal of Applied Mechanics and Engineering* **4** (2009) 415.
[19] R. Kumar, G. Partap // *Thai Journal of Mathematics* **8** (2010) 73.
[20] A.S. El-Karamany // *Journal of Thermal Stresses* **34(9)** (2011) 985.
[21] M.K. Mondal, B. Mukhopadhyay // *International Journal of Applied Mathematics and Mechanics* **9(17)** (2013) 51.
[22] R. Kumar, K.D. Sharma, S.K. Garg // *Materials Physics and Mechanics* **15** (2012) 135.
[23] R. Kumar, V. Chawla, I.A. Abbas // *Journal of Theoretical and Applied Mechanics* **39(4)** (2012) 313.
[24] J.N. Sharma, D.K. Sharma, S.S. Dhaliwal // *Open Journal of Acoustic* **2** (2012) 12.
[25] S. Sharma, K. Sharma, R.R. Bhargava // *Materials Physics and Mechanics* **16** (2013) 144.
[26] R. Kumar, K.D. Sharma, S.K. Garg // *Advances in Acoustics and Vibration* **2014** (2014) 846721.
[27] R. Kumar, M. Kaur, S.C. Rajvanshi // *Journal of Engineering Physics and Thermophysics* **87(2)** (2014) 295.
[28] R. Kumar, M. Kaur // *Archive of Applied Mechanics* **84** (2014) 571.
[29] A. Magana, R. Quintanilla // *Journal of Mathematical Analysis and Applications* **412(1)** (2014) 109.
[30] M. Svanadze // *Journal of Thermal Stresses* **37(3)** (2014) 253.
[31] H. Lord, Y. Shulman // *Journal of Mechanics and Physics of Solids* **15** (1967) 299.
[32] A.C. Green, K.A. Lindsay // *Journal of Elasticity* **2** (1972) 1.
[33] D.V. Strunin // *Journal of Applied Mechanics* **68** (2001) 816.
[34] W.S. Slaughter, *The Linearized Theory of Elasticity* (Birkhauser, Boston, Cambridge, 2002).